Effects of long-term warming and enhanced nitrogen and sulfur deposition on microbial communities in a boreal peatland

Magalí Martí[1,2] Alexander Eiler[3,4,5], Moritz Buck[3], Stefan Bertilsson[3], Waleed Abu Al-Soud[6,7], Søren Sørensen[6], Mats B. Nilsson[8], Bo H. Svensson[1]

[1] Department of Thematic Studies – Environmental Change, Linköping University, Linköping, Sweden
[2] Department of Clinical and Experimental Medicine, Linköping University, Linköping, Sweden
[3] Department of Ecology and Genetics, Limnology and Science for Life Laboratory, Uppsala University, Uppsala, Sweden
[4] eDNA solutions, Environmental DNA and bioinformatics solutions, Mölndal, Sweden
[5] Department of Biosciences, Center for BioGeoChemistry in the Anthropocene, Section for Aquatic Biology and Toxicology, University of Oslo, Oslo, Norway
[6] Department of Biology, Section of Microbiology, University of Copenhagen, Copenhagen, Denmark
[7] Department of Clinical Laboratory Sciences, Jouf University, Qurayyat, Saudi Arabia
[8] Department of Forest Ecology & Management, Swedish University of Agricultural Sciences, Umeå, Sweden

Corresponding author: Magalí Martí, magali.marti.genero@liu.se.

Abstract

With ongoing environmental change, it is important to understand ecosystem responses to multiple perturbations over long time scales at *in situ* conditions. Here, we investigated the individual and combined effects of 18 years of warming and enhanced nitrogen and sulfate deposition on peat microbial communities in a nutrient-poor boreal mire. The three perturbations individually affected prokaryotic community composition, where nitrogen addition had the most pronounced effect, and its combination with the other perturbations led to additive effects. The functional potential of the community, characterized by shotgun metagenomics, was strongly affected by the interactive effects in the combined treatments. The responses in composition were also partly reflected in the functional gene repertoire and in altered carbon turnover, i.e. an increase of methane production rates as a result of nitrogen addition and a decrease with warming. Long-term nitrogen addition and warming-induced changes caused a shift from *Sphagnum*-dominated plant communities to vascular plant dominance, which likely transact with many of the observed microbial responses. We conclude that simultaneous perturbations do not always lead to synergistic effects, but can also counteract and even neutralize one another, and thus must be studied in combination when attempting to predict future characteristics and services of peatland ecosystems.

Keywords Microbial diversity, 16S rRNA, metagenome, peatland, climate change, nitrogen

Introduction

Despite key roles of microbial communities in controlling carbon and nutrient dynamics within ecosystems, few studies have addressed effects of multiple drivers (e.g. anthropogenic stressors) on microbial taxonomic diversity and the associated genome-encoded traits underpinning realized ecosystem services (cf. Castro et al. 2010, Li et al. 2013, Andresen et al. 2014, Shen et al. 2014, Contosta et al. 2015). Given the multitude of human-derived disturbances, including climate change and atmospheric deposition of anthropogenic emissions, it is important to understand microbial community responses to multiple and parallel changes in the environment. Microorganisms will potentially react to such external impacts by shifting their community composition and function. This may lead to ecosystem structure repercussions causing feedbacks on e.g. the climate system via changes in greenhouse gas turnover and other ecosystem-scale processes. However, altered ecosystem services resulting from microbial community shifts may also be attenuated by functional redundancy within the community, assuming that many species are able to mediate the same functions in the ecosystem (Lawton & Brown 1993, Nielsen et al. 2011, Tully et al. 2018).

Microbial metabolism is central for most ecosystem services due to its central role in the turnover of essential nutrients and biogeochemical cycles (Martiny et al. 2015). For example, changes in the abundance of key microbial taxa able to produce or oxidize methane will influence the rate of methane emissions from various ecosystems that feature relevant redox conditions (McCalley et al. 2014). It is now tractable to characterize such genome-encoded functional traits with community-scale metagenome sequencing.

In situ manipulation experiments are well suited to test the responses of ecosystems and their microbial communities to various disturbance scenarios. Except for long-running trials in agricultural and forestry systems (Ramirez et al. 2010, Fierer et al. 2012, Leff et al. 2015, Zhou et al. 2015, Boot et al. 2016, Zeng et al. 2016), generally, *in situ* manipulations of soil

ecosystems have mainly been conducted over short- to intermediate-length time periods, e.g. between 1 to 5 years. Thus, several such short time field studies on effects of nitrogen amendment and warming on diversity, function and abundance of microbial communities have been reported (Castro et al. 2010, Li et al. 2013, Andresen et al. 2014, Shen et al. 2014, Contosta et al. 2015). Yet, to identify environmental responses over ecologically relevant timescales, while at the same time accounting for short-term disturbance effects, long-term (at least decadal) field experiments are needed (Rinnan et al. 2007, Eriksson et al. 2010a, Contosta et al. 2015). Moreover, as all ecosystems are influenced by multiple stressors, we need to understand how interactive effects of multiple effectors (synergistic or antagonistic perturbations) influence microbial communities if we are to robustly predict ecosystem responses to global warming, changes in atmospheric nutrient deposition and anthropogenic pollution in general.

Ever since the last de-glaciation, northern peatlands have played an important role in the global carbon balance, and are currently estimated to hold 30% of the global soil carbon, i.e. carbon stocks estimated at 270 - 600 Pg of organic C (Gorham 1991, Turunen et al. 2002, Yu 2012). Due to slow rates of microbial decomposition, there is an imbalance between primary production and degradation in these ecosystems. Thus, undisturbed peatlands are generally contemporary net sinks of carbon dioxide (CO_2), while at the same time being significant sources of methane (CH_4) to the atmosphere (Roulet et al. 2007, Nilsson et al. 2008, Turetsky et al. 2014). Therefore, the impact of the predicted global climate change and atmospheric nitrogen (N) and sulfate (S) deposition on the peatland net ecosystem carbon balance (NECB) is a topic of major concern (Granberg et al. 2001, Galloway et al. 2004, Gauci et al. 2004, Phoenix et al. 2012).

Increased N availability is known to strongly affect plant species composition and performance of different plant functional types in peatlands (Damman 1988, Bridgham et al.

1996, Eppinga et al. 2010, Limpens et al. 2011) as N is often a limiting nutrient (Wang & Moore 2014). This is clearly demonstrated by the shift towards vascular plant-dominated vegetation in the long-term high N deposition experiment at Degerö Stormyr (Wiedermann et al. 2007, Eriksson et al. 2010a, Eriksson et al. 2010b). As a result, methane emissions increased in response to the enhanced N deposition (Eriksson et al. 2010b), whereas warming led to a decrease in methane production, oxidation and emissions (Eriksson et al. 2010a, Eriksson et al. 2010b).

It has been argued that novel mechanistic insights on biogeochemical dynamics can be obtained by studying peat microbial community composition and function, and that such information can further improve predictions of ecosystem responses to global change (Bragazza et al. 2015). To investigate the isolated and interactive effects of warming, N and S deposition on the peat microbial community and function, we applied high throughput sequencing approaches to peat samples collected after 18 years of continuous *in situ* field manipulation. We took advantage of a full factorial experimental design that was established at Degerö Stormyr in 1995, consisting of nitrogen (NH_4NO_3) and sulfate (Na_2SO_4) amendments and warming (plots scale green-house covers) simulating the predicted effect of climate change (Granberg et al. 2001). Overall, simulated increased N deposition had the most pronounced effect on bacterial as well as archaeal communities. Multiple stressors interacted to give responses at the level of taxonomic and functional diversity, which influenced the functional potential of the ecosystem with regards to methane production, sulfate reduction, nitrate reduction and polymer hydrolysis. Thus, our experiment emphasizes the need to study the effects of climate change on microbial communities in the context of multiple environmental changes and anthropogenic-induced perturbations.

Materials and Methods

Site description and peat samples collection

Peat samples were collected from a full factorial experimental design in a *Sphagnum*-dominated oligotrophic area at Degerö Stormyr, in North Sweden (64°11'N, 19°33'E, altitude 270 m above sea level). Briefly, the experimental site is a boreal oligotrophic minerogenic mire, with a surface water pH of ~4.5. The climate of the reference period (1961-1990) was characterized by a mean annual precipitation of 523 mm, a mean annual temperature of 1.2°C, and a mean July and January temperatures of 14.7°C and -12.4°C, respectively. Average weather conditions during 2001-2012 were as follows (Peichl et al. 2014): annual and growing season air temperatures 2.3°C and 11°C, respectively, annual and growing season precipitation of 666 and 395 mm, respectively, and the growing season mean water table level at 14 cm below peat surface. The dominant vascular plants are *Eriophorum vaginatum* (L), *Andromeda polifolia* (L). and *Vaccinium oxycoccos* (*L.*). The dominant moss species are *Sphagnum balticum* (Russ) C. Jens. and, *S. lindberghii* (Schimp). The experiment was established in 1995 (Granberg et al. 2001) and was conducted according to a full factorial experimental design including two levels of nitrogen (N) i.e. ambient (low-level) at 2 kg N ha^{-1} yr^{-1} and amendment (high-level) of NH_4NO_3 to reach a deposition at a level of 30 kg N ha^{-1} yr^{-1}, two levels of sulfur (S) i.e. ambient at 3 kg S ha^{-1} yr^{-1}, and amendment of Na_2SO_4 to a level of 20 kg S ha^{-1} yr^{-1}, and two levels of greenhouse (GH) treatment, i.e. high level GH with a transparent cover or ambient (low level) of GH i.e. without a cover. Each experimental combination was performed in duplicate. The elevated levels of N and S correspond to the annual deposition amounts in southwest Sweden at the time for the start of the experiment. For a detailed description of the site and experimental design see Granberg et al. (2001), and for details on treatment effects on vegetation composition see Wiedermann et al. (2007). One peat core (0-40cm) was collected from each field plot (n=16) on August 14th and 15th 2013. From each core, 5 cm^3 of peat were subsampled at five depths from below the *Sphagnum*

148 surface: 7-11 cm (A), 11-15 cm (B), 15-19 cm (C), 19-23 cm (D) and 23-27 cm (E). The
149 samples were stored in 50 mL sterile tubes containing 2 mL of LifeGuard™ Soil Preservation
150 Solution (MoBio Laboratories, Hameenlinna, Finland), and kept at room temperature (<20°C)
151 for at most 24 hours before freezing at -20°C.
152
153 **Sample preparation**
154 Before extraction, peat samples were thawed over night at 4°C and centrifuged at 2500 x g for
155 5 min. Total RNA and DNA were co-isolated from 2 g wet peat and recovered in 50 µl using
156 the RNA PowerSoil® Total RNA Isolation Kit together with the RNA PowerSoil® DNA
157 Elution Accessory Kit (MoBio Laboratories), according to manufacturer's instructions.
158 Extract concentrations were measured with the Quant-iT RNA HS assay and the Quant-iT
159 dsDNA HS assay kits together with the Qubit fluorometer (Invitrogen, Lidingö, Sweden). The
160 RNA and DNA extraction yields ranged 2.5 - 122 ng μl^{-1} and 0.5 - 600 ng μl^{-1}, respectively.
161 Two extractions from each sample were performed and combined after extraction. RNA
162 combined extractions were concentrated using the RNA Clean & Concentrator™-25 (Zymo
163 Research, Taby, Sweden), in accordance with the manufacturer's instructions. DNA was
164 concentrated by the use of a Vacufuge® vacuum concentrator 5301 (Eppendorf, Horsholm,
165 Denmark). DNA residues were removed from the concentrated RNA extracts by digestion
166 using 2U TURBO DNase (Ambion-Life Technologies, Stockholm, Sweden) for 1 h at 37°C
167 and according to manufacturer's instructions. Reverse transcription was performed adding 2
168 µl of DNAse-treated RNA to 17 µl reaction mixture containing 1X Expand Reverse
169 Transcriptase Buffer (Roche Diagnostics, Mannheim, Germany), 10mM of Dithiothreitol
170 (DTT) solution (Roche diagnostics), 5 mM of dNTPs (New England BioLabs Inc., Glostrup,
171 Denmark) and 250 nM of random hexamers (TAG Copenhagen A/S, Copenhagen, Denmark).
172 After 2 min incubation at 42°C in a DNA engine DYAD™ Peltier Thermal Cycler (MJ

researchBio-Rad Laboratories, Hercules, CA), 1 µl of Expand Reverse Transcriptase (Roche Diagnostics) was added to the mixture and incubated at 42°C for 40 min followed by 30 min at 50°C and 15 min at 72°C. RNA template addition was in the range of 8 – 300 ng.

Amplicon sequencing and sequences analysis

PCR amplification of the bacterial and archaeal 16S rRNA and 16S rRNA gene V4 region fragment was performed using the primer pair 515F/806R (Caporaso et al. 2012) for all samples (Table S1). The primers used for amplicon sequencing of the 16S rRNA gene were selected following the Earth Microbiome Project recommendation (http://www.earthmicrobiome.org/emp-standard-protocols/) representing the best choice at the initiation of the study. The primer 806R was previously modified to cover most available sequences in Genbank by Sundberg et al. (2013). More recently, these primers have been shown to be biased against Crenarcheota (Hugerth et al. 2014). Three µl of template (cDNA or DNA) were added to a 20 µl-reaction mixture, consisting of 1X AccuPrime PCR Buffer II (Invitrogen), 0.2 U of AccuPrime *Taq* DNA Polymerase High Fidelity (Invitrogen) and 500 nM of each primer. The PCR assay was performed in a DNA engine DYAD™ Peltier Thermal Cycler (Bio-Rad Laboratories) with the following conditions: 94°C for 2 min, followed by 35 cycles of 94°C for 20 s, 56°C for 30 s and 68°C for 40 s, and a final extension at 68°C for 5 min. PCR products were visualized on a 1% agarose gel. A second PCR using the same primers including adapters and indexes was performed under the same conditions as the previous PCR with the number of cycles reduced to 15. PCR amplicons were purified using Agencourt AMPure XP (Agencourt Bioscience Corporation, MA, USA) and concentration was measured using PicoGreen assay according to manufacturer's protocol (Invitrogen). To ensure equal representation of each sample, 50 ng of each 16S rRNA and rRNA gene purified sample amplicons were pooled together before sequencing. Then the

198 pooled mixture was purified and concentrated using the DNA Clean & Concentrator™-5
199 (Zymo Research) followed by quantification with the Quant-iT dsDNA HS assay kit and the
200 Qubit fluorometer (Invitrogen). A paired-end 250-bp sequencing run was performed using the
201 Illumina MiSeq instrument according to the MiSeq™ Reagent Kit v2 Preparation Guide
202 (Illumina, Inc., San Diego, CA, USA).
203 Raw read data was processed using the ILLUMITAG pipeline (Sinclair et al. 2015). In
204 short, the read pairs from the 16S rRNA gene and 16S rRNA were demultiplexed and joined
205 using the PANDAseq software v2.4 (Masella et al. 2012). Next, assembled reads (from here
206 referred to as "reads") that did not have the correct primer sequences at the start and end of
207 their sequences were discarded. Reads were then filtered based on their PHRED scores.
208 Chimera removal and OTU (operational taxonomic unit) clustering at 1% sequence
209 dissimilarity was performed by pooling all reads from all samples (but separately for genomic
210 16S rRNA and 16S rRNA) together and applying the UPARSE algorithm v7.0.1001 (Edgar
211 2013). Here, any OTU containing less than two reads was discarded. Each OTU was
212 subsequently taxonomically classified by operating a similarity search against the SILVAmod
213 databases and employing the CREST assignment resource (Lanzen et al. 2012). Finally,
214 plastid and mitochondrial OTUs were removed.
215 We obtained a total of 4 965 761 sequence reads (including both, the 16S rRNA and 16S
216 rRNA gene), from which 4 811 127 sequences belonged to the domain Bacteria and 15 444 to
217 the domain Archaea. Bacterial and archaeal sequences were analysed together as the
218 combined prokaryote community. Prior to estimating alpha diversity, to minimize the impact
219 of varying sequencing depth among the samples, the reads were rarefied to 5315 and 5455
220 sequences per sample for RNA and DNA, respectively. Three RNA and 2 DNA samples were
221 excluded due to low number of sequences (Table S1). Prokaryote richness and evenness
222 (alpha diversity) were estimated using the Chao1 and Pileou's indices, where a Pielou index

of 1 represents absolute evenness. Prior to beta-diversity analyses and to avoid excluding samples, the number of reads for individual samples were rarefied to the minimum number of sequences observed per sample: 3331 and 3348 sequences for 16S rRNA and the 16S rRNA gene, respectively.

Shotgun metagenome sequencing, assembly and annotation

Shotgun sequencing was performed on samples from depths B (11-15 cm) and D (19-23 cm), (Table S1). Depth B corresponds to the level around which the mean growing season water table occurs, which is the depth horizon with the most metabolic activity. Depth D is below the growing season water table level fluctuations and, thus, continuously anoxic. 1ng of each DNA sample (from B and D depths) were used for tagmentation using the Nextera XT (Illumina, Inc., San Diego, CA, USA), according to manufacturer's instructions. Tagmented samples were purified using Agencourt AMPure XP (Agencourt Bioscience Corporation, MA, USA). Purified samples were visualized on a 1% agarose gel to ensure the libraries range was within 300-1000 bp. Libraries concentrations were measured with Quant-iT dsDNA HS assay and the Qubit fluorometer (Invitrogen). To ensure equal representation of each sample, 10 ng of each sample library were pooled together before sequencing. A paired-end 150-bp sequencing run was performed using the Illumina Rapid Run on an Illumina HiSeq 2500 platform (Illumina, Denmark), according to manufacturer's instructions.

The obtained reads were quality-trimmed using Sickle (Joshi & Fass 2011), and all samples were co-assembled with a range of k-mer values (from 31 to 101 with increments of 10) using Ray (Boisvert et al. 2012). The resulting assemblies were subsequently fragmented *in silico* into successive sequences of 2000 base pairs overlapping by 1900 bp and were then merged using 454 Life Sciences's software Newbler (Roche, Basel, Switzerland) as previously described (Hugerth et al. 2015). The clean reads of all samples were mapped to the

merged assembly using Bowtie (Langmead & Salzberg 2012) after processing with SAMtools (Li et al. 2009). Duplicates were removed using Picard (Broad Institute, Cambridge, MA, USA). Finally, coverage was computed using BEDTools (Quinlan & Hall 2010). PFAM (protein families) annotation was performed using HMMer (Eddy 2011) using the PFAM A database (Finn et al. 2014). For each sample, the coverage of all detected PFAMs was normalized by dividing it by the mean coverage of a set single copy PFAMs (Rinke et al. 2013) in order to compile the coverage in a "per genome equivalent" form. PFAM tables standardized to genome equivalents were resampled by removing PFAMs with smaller genome equivalents than the highest minimum genome equivalent ($6.9x10^{-4}$) of sample NxGH.

Statistical analyses

The multifactorial experiment consists of three treatment factors at two levels (2^3-design) with field duplicates for each treatment. Thus, the statistical evaluation is based on n=8 for the main factors N, S and GH and n=4 for the 2-way interaction treatments (NxS, NxGH and SxGH) and n=2 for the 3-way interaction (NxSxGH), see Table S2 for the treatment effect evaluation matrix. After 10 years of treatment, the addition of N had significantly reduced the distance between the mire surface and the growing season average water table (Eriksson et al. 2010b). To account for this gradual change and the inherent variation among the plots, the sampled depths were classified according to their positions relative to the average growing seasonal water table level within each plot as given by (Eriksson et al. 2010a), (Table S3). This resulted in three different depth horizons: an upper layer above the growing season mean water table level, which will be the most oxic of the three (AWT), a layer around the growing season mean water table level (WT) and a third layer below the growing season mean water table level characterized by permanent anoxic conditions (BWT).

ANOVA was applied to test for the effects of the treatments on the prokaryotic alpha-diversity. Permutation analysis of variance (PERMANOVA) was applied to test the hypothesis that the prokaryotic community composition and its functional potential differed among the treatments. To assess whether the microbial composition turnover in the treatment plots followed the same direction, ordination by non-metric multidimensional scaling was used. In order to understand how the response of the microbial community was distributed across the different phyla, we used the integrated occurrence of each phylum along the entire peat profiles and calculated the average change in their relative abundance derived from the 16S rRNA for the high treatment levels in relation to their corresponding low levels. The phyla were sorted according to their relative abundance in the combined 16S rRNA dataset and are presented with either positive or negative responses to the treatments. In this context, it should be noted that changes at the phylum level might only be a rough representation of changes in the functional capacity of the communities. To assess individual metabolic traits in the different treatments, we applied generalized linear models (GLMs) on genome equivalent standardized PFAMs across the different treatments. We focused on PFAMs predicting key enzymes involved in the anaerobic degradation of soil organic matter, as well as methanotrophy (Table S4). The resulting differentially abundant categories (taxa or functional subsystems) among samples were identified based on $p<0.05$ and false discovery rate was estimated (Benjamini & Hochberg 1995). A distance-based redundancy analysis (db-RDA) was applied to explore possible multiple linear correlations between the microbial community composition and the vegetation composition previously reported (Eriksson et al. 2010b). Correspondence between the different data sets was investigated using procrustes superimposition combined with a randomisation test (Peres-Neto & Jackson 2001). Bray-Curtis distance was used when a distance matrix was required applying 999 permutations. The statistic discrimination throughout the analyses was at a significance level of 0.05.

298

299 **Nucleotide sequence accession numbers**

300 The sequence data generated in this study was deposited to the NCBI Sequence Read Archive
301 and is accessible through accession number PRJEB14741.

302

303 **Results**

304 **Microbial community composition**

305 High throughput sequencing data was used to follow prokaryotic community composition and
306 metabolic traits responding to the perturbations in the factorially designed experiment. High
307 concordance was observed between the 16S rRNA gene and 16S rRNA-derived community
308 compositions, as determined by procrustes superimposition ($p = 0.001$, $R = 0.9$; Table S5).
309 Comparisons of treatments revealed that the three main factors (nitrogen (N), sulfate (S) and
310 warming (GH)) significantly affected the prokaryote community compositions (i.e. the beta-
311 diversity; Table 1). In all cases, enhanced inorganic N deposition (high level) significantly
312 affected the community composition at all depth horizons, contributed the most to the
313 explained variance (Table 1), and showed the highest degree in dissimilarity compared to the
314 ambient N (low level) (Fig. 1). In contrast to beta-diversity describing compositional changes
315 (as determined by Bray-Curtis distances), alpha-diversity assessed as prokaryotic richness and
316 evenness estimates, revealed only few significant responses to the perturbations (Table 1).
317 Richness increased with the warming effect, while evenness overall decreased as a result of
318 all the perturbations (Fig. S1).

319 The combined perturbations (i.e. high levels of NxS, NxGH, SxGH and NxSxGH) caused
320 significant interactive effects that shifted the prokaryotic community (i.e. the beta-diversity:
321 Table 1 and Fig. 1). For example, the 16S rRNA gene-derived prokaryotic community (beta-
322 diversity) response to warming increased with enhanced N deposition in the two upper

horizons, while enhanced S deposition significantly increased the warming effect below the water table. Such synergistic effects were also observed when combining N and S deposition. While treatment interactions appeared to be additive as based on the observation that the dissimilarity among communities increased when applying multiple perturbations, their directionality were not consistent (Fig. 1 and Fig. S2). This implies that communities experiencing impacts from multiple perturbations do not merely change in a linear fashion based on combinations of individual perturbations, but are emerging in response to the establishment of unique communities for a particular combination of effectors. For example, enhanced N deposition combined with another perturbation (NxS, NxGH and NxSxGH) tended to cause greater community changes compared to the single perturbations at the two upper layers (Fig. 1a and 1b). Below the growing season mean water table (BWT) horizon, the amplitudes of the community composition responses in comparison to the control were similar for all perturbations (Fig. 1c).

There was concordance between beta diversity of the plant vegetation, derived from Wiedermann et al. (2007), and the peat prokaryote community at all three depth horizons, as revealed by procrustes superimposition ($p = 0.001$, $R = 0.4 - 0.7$; Table S5). In addition, db-RDA analyses revealed that the prokaryotic composition in the treatments receiving NH_4NO_3 (high N) were positively correlated with the relative abundance of the dominant vascular plants (*E. vaginatum, A. polifolia and V. oxycoccus*) and negatively correlated with total *Sphagnum* and *S. balticum* coverage (Fig. S3).

Bacterial and archaeal 16S rRNA gene sequences and expressed 16S rRNA sequences were classified into 31 and 33 phyla, respectively. The main phyla were Verrucomicrobia and Acidobacteria accounting respectively for 39% and 26% of the reads in the 16S rRNA gene-derived community, while Acidobacteria accounted for 36% and Proteobacteria for 23% of the reads in the 16S rRNA-derived community. The abundance of the different phyla was

clearly and differentially affected by the perturbations (Fig. 2). For example, the phyla Acidobacteria, Firmicutes, and Armatimonadetes decreased in relative abundance in response to all the treatments, while Chlorobi, Euryarchaeota, Fibrocateretes, and Tenericutes showed the opposite response. Verrucomicrobia and Actionabacteria increased in response to the main N effect and decreased in the other treatments, while candidate phylum BD1-5 had the opposite response. Cyanobacteria and Fusobacteria, increased in response to the main warming effect while for all the other treatments decreased and disappeared, respectively. Dictyoglomi increased with N, GH and NxGH while disappeared with all the other treatments. Thaumarchaetoa and candidate division TM7 disappeared with warming while increased with N, S and NxS perturbations.

Microbial metabolic traits

In addition to responses in the composition of operational taxonomic units and taxonomic groups at the phylum level, we assessed the treatment responses with regards to genome-encoded metabolic traits from shotgun metagenomic data. In total, protein-coding genes matching 4957 protein families (PFAMs) were found from the 31 metagenomes. Overall responses in the functional potential as determined by estimating Bray-Curtis distances revealed that only enhanced N deposition (high -N) caused a significant shift in functional attributes, and this was only observed below the water table (Table 1). There was also a significant interactive effect when warming and increased S deposition perturbations were combined (Table 1).

Moreover, we specifically searched for marker genes related to key steps in the anaerobic degradation of organic matter (e.g. nitrate- and sulfate reduction, hydrolysis, fermentation, methanogenesis) and aerobic methane and ammonia oxidation (Table S4). From 1057 possible responses at each depth horizon, merely 24 significant responses ($p<0.05$; FDR of

373 0.30) could be extracted from above the growing season mean water table (AWT), while the
374 corresponding number in samples from below the growing season mean water table (BWT)
375 was 30. At the AWT horizon, a few genes encoding for key steps in processes such as
376 methanogenesis, sulfate reduction, nitrate reduction, sulfur oxidation, nitrogen fixation,
377 syntrophy and hydrolysis, responded significantly to the experimental treatments (Fig. 3a).
378 The majority of significant responses were connected to the 2-way interactive terms (NxS,
379 NxGH and SxGH). Marker genes for methanogenesis significantly decreased in response to
380 the main effects (N, S and GH), with amplification effects connected to the NxSxGH
381 interaction, while they increased in response to the 2-way interactive terms. Genes encoding
382 for proteins involved in dissimilatory sulfate reduction increased under enhanced S
383 deposition, with amplification effects under the three-way perturbation and a decrease in the
384 response when combined with warming or N.
385 At the BWT horizon, only a few genes encoding for methanogenesis, sulfate reduction,
386 nitrate reduction, sulfur oxidation, syntrophy, and hydrolases responded significantly to the
387 treatments. At this horizon the majority of the responses were connected to warming and
388 enhanced S deposition, both resulting in a decrease of the different metabolic potentials,
389 except for sulfate reduction that increased with the elevated S deposition (Fig. 3b). However,
390 the few significant effects of the 2- and 3-way interactions with S or GH seemed to counteract
391 these responses, resulting in an increase of the respective metabolic traits. For example,
392 marker genes for methanogenesis, as observed for the AWT horizon, significantly decreased
393 in response to the individual S and GH effects but increased in response to the NxS and
394 NxSxGH perturbations. Genes encoding for hydrolases were the most affected among the
395 studied metabolic traits, and mainly decreased with warming and enhanced S deposition as
396 well as with simultaneous increase in N and S depositions.
397

398 **Co-variations between ecosystem functions and genetics in the light of perturbations**

399 Taxonomic composition and genome-encoded traits were tightly coupled ($p = 0.001$, $R =$
400 0.87; Table S5). The previously reported realized methane production (Eriksson et al. 2010a),
401 and the taxonomic composition data at 16S rRNA level were strongly related to each other
402 across the different treatments and depth horizons (Table 2). However, genome-encoded
403 functional traits as assessed from shotgun metagenomic data, including marker genes for
404 methanogenesis and methanotrophy, did not correspond with measured function (i.e. methane
405 production and oxidation; data no shown).
406

407 **Discussion**

408 The long field experiment at the Degerö Stormyr peatland was established to investigate the
409 effects of increased nitrogen (N) and sulfur (S) deposition as well as warming on methane and
410 carbon dynamics in boreal oligotrophic mires (Granberg et al. 2001). Here we report on
411 interactive long-term effects after 18 years of multiple perturbations on prokaryotic taxonomic
412 diversity and genome-encoded traits, as well as their relationship with ecosystem-scale
413 processes of interest (*i.e.* methane cycling, organic matter degradation and plant composition).
414 The microbial taxonomic composition largely corresponds with results from previous studies
415 of peatlands (Lin et al. 2012, Serkebaeva et al. 2013, Tveit et al. 2013). Thus, the proportion
416 of archaeal sequences at 0.3% of total prokaryotic sequences was in the range of what has
417 previously been observed for peat ecosystems (Tveit et al. 2013 and references therein). We
418 also show that where vascular plants (*E. vaginatum, A. polifolia and V. oxycoccus*) replaced
419 *Sphagnum* under N amendments (Wiedermann et al. 2007, Eriksson et al. 2010b), also
420 prokaryotic communities shifted in composition in response to N additions. The concordance
421 between beta-diversity of the plant vegetation composition derived from Wiedermann et al.
422 (2007) and the composition of the peat prokaryote community, confirms the tight coupling

423 between vegetation and microbes in the peat biome. The enrichments of roots at 10-15 cm
424 into the peat vertical profile (Olid et al. 2017) likely play an essential role for this
425 development by causing changes in organic matter composition and availability. The high
426 level of N induced shifts in relative abundance among many phyla reported to harbour
427 hydrolytic enzymes (Juottonen et al. 2017 and therein), i.e. increases in Proteobacteria and
428 Actinobacteria, while Acidobacteria, Planctomycetes, and Bacteroidetes decreased.
429 Interestingly, the decrease in Acidobacteria concomitantly with the relative increase in
430 Proteobacteria may indicate a shift from the naturally nutrient poor conditions in the nutrient
431 poor fen to more nutrient rich conditions because of the N amendment. In agreement with
432 this, Lin et al. (2012) observed a higher abundance of Proteobacteria in rich fens compared to
433 nutrient poor bogs. Since both phyla contain anaerobic carbohydrate polymer degrading
434 representatives, these phyla may replace one another (cf. Schmidt et al. 2015) as result of
435 changes in the type of carbohydrates supplied by the different plant communities forming the
436 peat. The decrease in Cyanobacteria may reflect the decrease in *Sphagnum* abundance.
437 Cyanobacteria occur in the hyalinic cell of the Sphagna lumena, where they have been shown
438 to perform dinitrogen fixation (cf. Granhall & Selander 1973, Granhall & von Hofsten 1976,
439 Berg et al. 2013). In addition to the taxonomic composition, also the genome-derived
440 functional potential (PFAMs) was related to the composition of the vegetation. As such, our
441 results fit the framework developed in studies of other soils subject to long-term N addition
442 experiments, both with regards to microbial community composition and functional potential
443 (Ramirez et al. 2010, Fierer et al. 2012, Leff et al. 2015, Zhou et al. 2015, Boot et al. 2016,
444 Zeng et al. 2016), including grasslands, agricultural fields, agricultural black soils, and
445 subalpine forests. For these systems, there is a consistent view that the shifts in microbial
446 community composition and their metabolic functionality is due to the soil-plant-microbe
447 interactions driven by N loading.

448 The significant relationships between prokaryotic community composition and methane
449 oxidation and production, further emphasize the role of plant-prokaryotic interactions in
450 regulating methane emissions. This is corroborated by the fact that all N amended to the plots
451 is retained in the organic fraction of the peat (Eriksson 2010). However, responses in the
452 overall set of genes, as well as the specific marker genes for methanogenesis and
453 methanotrophy, did not match the patterns of observed methane production and consumption
454 rates previously reported (Eriksson et al. 2010a). There are multiple possible explanations for
455 the lack of correspondence, including an actual decoupling between gene abundance and their
456 expression (Roling 2007, Freitag & Prosser 2009) or a high variability of the genomic content
457 between individual samples. Also, temporal variation could play a role, as methane processing
458 rates and genetic data were obtained during different years and locations within the treatment
459 plots.
460 Similar to the elevated N deposition, also warming led to changes in prokaryotic
461 community composition, supporting earlier findings of decreased methane production and
462 emission rates while methane oxidation was unaffected (Eriksson et al. 2010a, Eriksson et al.
463 2010b). Thus, the relative abundance of genes involved in methanogenesis decreased in
464 response to warming, while other metabolic traits such as methanotrophy were largely
465 unaffected. The observed decrease in the methanogenic potential may be explained by lower
466 input of easily degradable organic matter to the anoxic zone due to oxygen-exposure in the
467 upper layers with higher temperature (Nilsson & Öquist 2009). Thus, the organic matter will
468 be more recalcitrant when it is transferred into the permanent anoxic layer. In favour of this
469 explanation, there was a decrease in the hydrolytic potential below the water table level
470 pinpointing to a lower degradability of the biopolymers at these strata.
471 The enhanced S deposition affected the microbial taxonomic composition at the water table
472 and the anoxic horizons. Although S amendment in the field did not have any effects on

473 methane emissions, laboratory incubations of the methane producing-layers have shown a
474 decrease in methane production by 55% in response to S amendments (Eriksson et al. 2010a,
475 Eriksson et al. 2010b). This observation is supported by our results that the relative abundance
476 of genes involved in methanogenesis were lower in the S-supplied plots. Below the water
477 table, the observed decrease in hydrolytic and syntrophic potential combined with an increase
478 of sulfate reduction potential, imply that organic matter degradation resulted in lower amounts
479 of metabolic fermentation intermediates and H_2 available for methanogenesis.
480 Above the water table, the sulfate reduction potential increased concomitantly with the
481 observed decrease in methanogenic potential as expected from the thermodynamic constraints
482 (Abram & Nedwell 1978, Kristjansson et al. 1982). Some of the sulfide generated in this
483 process is likely emitted to the atmosphere at the prevailing low pH, while experimentally
484 added S over the years has contributed to a 50% larger S-pool under ambient climate and to a
485 ~15% larger S-pool when combined with the greenhouse treatment (Granberg et al. 2001,
486 Åkerblom et al. 2013). A re-oxidation of this residual S-pool would result in a continuous
487 supply of oxidized sulfur compounds that would sustain sulfate reduction in these treatments.
488 The increase of the photosynthetic sulfur oxidizers, here represented by the phylum Chlorobi,
489 in response to essentially all perturbations and in particular the S amendments, supports the
490 presence of an internal sulfur cycle (Pester et al. 2010, Pester et al. 2012). Such a sulfur cycle
491 is suggested to be involved in the regulation of the ratio between carbon dioxide to methane
492 formation in peatlands (Pester et al. 2010, Pester et al. 2012).
493 The nitrogen applied has been shown to be completely retained for the duration of the
494 experiment in the form of nitrogenous organic matter (Eriksson 2010). Because of this, the
495 amendment of N to these highly nitrogen-limited systems is not expected to enhance the
496 occurrence of ammonia oxidation, dissimilatory nitrate reduction to ammonia or
497 denitrification. This is supported by the lack of any significant response of genes encoding for

498 these processes in the N-amended plots. However, the 16S RNA analysis revealed that phyla
499 hosting archaeal nitrifiers were present and increased in the plots with N addition. Especially,
500 the positive response by groups within the Thaumarchaeota that have been shown to oxidize
501 ammonia at very low levels, would potentially supply nitrite in the high-level N treatments.
502 However, any nitrite formed would likely be immediately reduced by means of
503 denitrification, anaerobic ammonium oxidation or assimilative or dissimilative reduction to
504 ammonia.
505

506 ## Conclusions

507 Experimental long-term treatments mimicking anthropogenic perturbations altered the
508 microbial communities at the taxonomic level and to some extent redistribute genes encoding
509 microbial metabolic profiles including changes in ecosystem-relevant traits, such as sulfate
510 reduction and methanogenesis, partly coinciding with expressed overall ecosystem functions.
511 The results from the 18-years field manipulation experiment emphasizes that interactive
512 effects of multiple anthropogenic perturbations on ecosystem services lead to idiosyncratic
513 and hard to predict disturbance-responses in natural microbial communities when studying
514 each perturbation in isolation. The observed additive effects of the treatments on community
515 composition and function emphasize the need for studying interactions among multiple
516 anthropogenic perturbations to understand ecosystem responses to climate change.
517

518 ## Acknowledgements

519 We thank Lucas Sinclair for bioinformatics support and the Uppsala Multidisciplinary Center
520 for Advanced Computational Science (UPPMAX) for the computational and storage
521 resources under projects b2014318. The project was mainly funded by the Swedish Research
522 Council (contract no: 621-2011-4901) and additional research grants from the Swedish

Research Council Formas to MN and SB and from the Swedish Research Council to AE, BS, MN and SB further supported the study. We are thankful to FEMS for the research fellowship (FRF 2014-1) award (MM).

References

Abram JW & Nedwell DB (1978) Inhibitionof Methanogenesisby Sulfphate Reducing Bacteria Competing for Transferred Hydrogen. Archives of Microbiology, 117: 89-92.

Åkerblom S, Bishop K, Björn E, Lambertsson L, Eriksson T & Nilsson M (2013) Significant interaction effects from sulfate deposition and climate on sulfur concentrations constitute major controls on methylmercury production in peatlands. Geochimica et Cosmochimica Acta 1-11.

Andresen LC, Dungait JA, Bol R, Selsted MB, Ambus P & Michelsen A (2014) Bacteria and fungi respond differently to multifactorial climate change in a temperate heathland, traced with 13C-glycine and FACE CO2. PloS One 9: e85070.

Benjamini Y & Hochberg Y (1995) Controlling the false discovery rate: a practical and powerful approach to multiple testing. Journal of the Royal Statistical Society Series B: 289-300.

Berg A, Danielsson Å & Svensson BH (2013) Transfer of fixed-N from N2-fixing cyanobacteria associated with the moss Sphagnum riparium results in enhanced growth of the moss. Plant and Soil: 271-278.

Boisvert S, Raymond F, Godzaridis E, Laviolette F & Corbeil J (2012) Ray Meta: scalable de novo metagenome assembly and profiling. Genome Biology 13: R122.

Boot CM, Hall EK, Denef K & Baron JS (2016) Long-term reactive nitrogen loading alters soil carbon and microbial community properties in a subalpine forest ecosystem. Soil Biology and Biochemistry 92: 211-220.

Bragazza L, Bardgett RD, Mitchell EA & Buttler A (2015) Linking soil microbial communities to vascular plant abundance along a climate gradient. New Phytologist 205: 1175-1182.

Bridgham SD, Pastor J, Janssens JA, Chapin C & Malterer TJ (1996) Multiple limiting gradients in peatlands: a call for a new paradigm. Wetlands 16: 45-65.

Caporaso JG, Lauber CL, Walters WA*, et al.* (2012) Ultra-high-throughput microbial community analysis on the Illumina HiSeq and MiSeq platforms. ISME J 6: 1621-1624.

Castro HF, Classen AT, Austin EE, Norby RJ & Schadt CW (2010) Soil microbial community responses to multiple experimental climate change drivers. Applied and Environmental Microbiology 76: 999-1007.

Contosta AR, Frey SD & Cooper AB (2015) Soil microbial communities vary as much over time as with chronic warming and nitrogen additions. Soil Biolology and Biochemistry 88: 19-24.

Damman A (1988) Regulation of nitrogen removal and retention in Sphagnum bogs and other peatlands. Oikos 51: 291-305.

Eddy SR (2011) Accelerated Profile HMM Searches. PLoS Computational Biology 7: e1002195.

Edgar RC (2013) UPARSE: highly accurate OTU sequences from microbial amplicon reads. Nature Methods 10: 966-988.

568 Eppinga MB, Rietkerk M, Belyea LB, Nilsson MB, De Ruiter PC & Martin JW (2010)
569 Resource contrast in patterned peatlands increases along a climatic gradient. Ecology
570 91: 2344-2355.
571 Eriksson T (2010) Boreal Mire Carbon Exchange. Dissertation. Serie: Acta Universitatis
572 agriculturae Sueciae, 1652-6880; 2010:62
573 Eriksson T, Öquist MG & Nilsson MB (2010a) Production and oxidation of methane in a
574 boreal mire after a decade of increased temperature and nitrogen and sulfur deposition.
575 Global Change Biology 16: 2130-2144.
576 Eriksson T, Öquist MG & Nilsson MB (2010b) Effects of decadal deposition of nitrogen and
577 sulfur, and increased temperature, on methane emissions from a boreal peatland. Journal
578 of Geophysical Research 115: 1 -13.
579 Fierer N, Lauber CL, Ramirez KS, Zaneveld J, Bradford MA & Knight R (2012) Comparative
580 metagenomic, phylogenetic and physiological analyses of soil microbial communities
581 across nitrogen gradients. ISME J 6: 1007-1017.
582 Finn RD, Bateman A, Clements J*, et al.* (2014) Pfam: the protein families database. Nucleic
583 Acids Research 42: D222-230.
584 Freitag TE & Prosser JI (2009) Correlation of methane production and functional gene
585 transcriptional activity in a peat soil. Applied and Environmental Microbiology 75:
586 6679-6687.
587 Galloway JN, Dentener FJ, D.G. C*, et al.* (2004) Nitrogen cycles: past, present, and future.
588 Biogeochemistry 70: 153-226.
589 Gauci V, Matthews E, Dise N, Walter B, Koch D, Granberg G & Vile M (2004) Sulfur
590 pollution suppression of the wetland methane source in the 20th and 21st centuries.
591 Proceedings of the National Academy of Sciences of the United States of America 101:
592 12583-12587.
593 Gorham E (1991) Northern peatlands: role in the carbon cycle and probable responses to
594 climatic warming. Ecological Applications 1: 182-195.
595 Granberg G, Sundh I, Svensson BH & Nilsson M (2001) Effects of temperature, and nitrogen
596 and sulfur deposition, on methane emission from a boreal mire. Ecology 82: 1982-1998.
597 Granhall U & Selander H (1973) Nitrogen fixation in a subarctic mire. Oikos 24: 8-15.
598 Granhall U & von Hofsten A (1976) Nitrogenase activity in relation to intracellular organisms
599 in Sphagnum Mosses. Physiologia plantarum 36: 88-94.
600 Hugerth LW, Larsson J, Alneberg J, Lindh MV, Legrand C, Pinhassi J & Andersson AF
601 (2015) Metagenome-assembled genomes uncover a global brackish microbiome.
602 Genome Biology 16: 279.
603 Hugerth LW, Muller EE, Hu YO, Lebrun LA, Roume H, Lundin D, Wilmes P & Andersson
604 AF (2014) Systematic design of 18S rRNA gene primers for determining eukaryotic
605 diversity in microbial consortia. PloS One 9: e95567.
606 Joshi NA & Fass JN (2011) Sickle: A sliding-window, adaptive, quality-based trimming tool
607 for FastQ files (Version 1.33) [Software]. Available at https://githubcom/najoshi/sickle.
608 Juottonen H, Eiler A, Biasi C, Tuittila ES, Yrjala K & Fritze H (2017) Distinct Anaerobic
609 Bacterial Consumers of Cellobiose-Derived Carbon in Boreal Fens with Different
610 CO2/CH4 Production Ratios. Applied and Environmental Microbiology 83: e02533-
611 02516.
612 Kristjansson JK, Schonheit P & Thauer RK (1982) Different Ks values for hydrogen of
613 methanogenic bacteria and sulfate reducing bacteria – an explanation for the apparent
614 inhibition of methanogenesis by sulfate. Archives of Microbiology, 131: 278-282.
615 Langmead B & Salzberg SL (2012) Fast gapped-read alignment with Bowtie 2. Nature
616 Methods 9: 357-359.

617 Lanzen A, Jorgensen SL, Huson DH, Gorfer M, Grindhaug SH, Jonassen I, Ovreas L & Urich
618 T (2012) CREST--classification resources for environmental sequence tags. PloS One 7:
619 e49334.
620 Lawton JH & Brown VK (1993) Redundancy in ecosystems. In: (Schulze ED & Mooney HA,
621 ed) Biodiversity and Ecosystem Function, Springer-Verlag Berlin, Germany, pp. 255-
622 270.
623 Leff JW, Jones SE, Prober SM*, et al.* (2015) Consistent responses of soil microbial
624 communities to elevated nutrient inputs in grasslands across the globe. Proceedings of
625 the National Academy of Sciences of the United States of America 112: 10967-10972.
626 Li H, Handsaker B, Wysoker A, Fennell T, Ruan J, Homer N, Marth G, Abecasis G, Durbin R
627 & Genome Project Data Processing S (2009) The Sequence Alignment/Map format and
628 SAMtools. Bioinformatics 25: 2078-2079.
629 Li Q, Bai H, Liang W, Xia J, Wan S & van der Putten WH (2013) Nitrogen addition and
630 warming independently influence the belowground micro-food web in a temperate
631 steppe. PloS One 8: e60441.
632 Limpens J, Granath G, Gunnarsson U*, et al.* (2011) Climatic modifiers of the response to
633 nitrogen deposition in peat-forming Sphagnum mosses: a meta-analysis. New
634 Phytologist 191: 496-507.
635 Lin X, Green S, Tfaily MM, Prakash O, Konstantinidis KT, Corbett JE, Chanton JP, Cooper
636 WT & Kostka JE (2012) Microbial community structure and activity linked to
637 contrasting biogeochemical gradients in bog and fen environments of the Glacial Lake
638 Agassiz Peatland. Applied and Environmental Microbiology 78: 7023-7031.
639 Martiny JB, Jones SE, Lennon JT & Martiny AC (2015) Microbiomes in light of traits: A
640 phylogenetic perspective. Science 350: aac9323.
641 Masella AP, Bartram AK, Truszkowski JM, Brown DG & Neufeld JD (2012) PANDAseq:
642 PAired-eND Assembler for Illumina sequences. BMC Bioinformatics 13.
643 McCalley CK, Woodcroft BJ, Hodgkins SB*, et al.* (2014) Methane dynamics regulated by
644 microbial community response to permafrost thaw. Nature 514: 478-481.
645 Nielsen UN, Ayres E, Wall DH & Bardgett RD (2011) Soil biodiversity and carbon cycling: a
646 review and synthesis of studies examining diversity-function relationships. European
647 Journal of Soil Science 62: 105-116.
648 Nilsson M & Öquist M (2009) Partitioning Litter mass Loss Into Carbon Dioxide and
649 Methane in Peatland Ecosystems. Geophysical Monograph 184: 131-144.
650 Nilsson M, Sagerfors J, Buffam I, Laudon H, Eriksson T, Grelle A, Klemedtsson L, Weslien
651 PER & Lindroth A (2008) Contemporary carbon accumulation in a boreal oligotrophic
652 minerogenic mire - a significant sink after accounting for all C-fluxes. Global Change
653 Biology 14: 2317-2332.
654 Olid C, Bindler R, Nilsson MB, Eriksson T & Klaminder J (2017) Effects of warming and
655 increased nitrogen and sulfur deposition on boreal mire geochemistry. Applied
656 Geochemistry 78: 149-157.
657 Peichl M, Sonnentag O & Nilsson MB (2014) Bringing color into the picture: using digital
658 repeat photography to investigate phenology controls of the carbon dioxide exchange in
659 a boreal mire. Ecosystems 18: 115-131.
660 Peres-Neto P & Jackson D (2001) How well do multivariate data sets match? The advantages
661 of a Procrustean superimposition approach over the Mantel test. Oecologia 129: 169-
662 178.
663 Pester M, Bittner N, Deevong P, Wagner M & Loy A (2010) A 'rare biosphere'
664 microorganism contributes to sulfate reduction in a peatland. ISME J 4: 1591-1602.

665 Pester M, Knorr KH, Friedrich MW, Wagner M & Loy A (2012) Sulfate-reducing
666 microorganisms in wetlands - fameless actors in carbon cycling and climate change.
667 Front Microbiol 3: 72.
668 Phoenix GK, Emmett BA, Britton AJ*, et al.* (2012) Impacts of atmospheric nitrogen
669 deposition: responses of multiple plant and soil parameters across contrasting
670 ecosystems in long-term field experiments. Global Change Biology 18: 1197-1215.
671 Quinlan AR & Hall IM (2010) BEDTools: a flexible suite of utilities for comparing genomic
672 features. Bioinformatics 26: 841-842.
673 Ramirez KS, Lauber CL, Knight R, Bradford MA & Fierer N (2010) Consistent effects of
674 nitrogen fertilization on soil bacterial communities in contrasting systems. Ecology 91:
675 3463-3470.
676 Rinke C, Schwientek P, Sczyrba A*, et al.* (2013) Insights into the phylogeny and coding
677 potential of microbial dark matter. Nature 499: 431-437.
678 Rinnan R, Michelsen A, Bååth E & Jonasson S (2007) Fifteen years of climate change
679 manipulations alter soil microbial communities in a subarctic heath ecosystem. Global
680 Change Biology 13: 28-39.
681 Roling WF (2007) Do microbial numbers count? Quantifying the regulation of
682 biogeochemical fluxes by population size and cellular activity. FEMS Microbiology
683 Ecology 62: 202-210.
684 Roulet NT, Lafleur PM, Richard PJH, Moore TR, Humphreys ER & Bubier J (2007)
685 Contemporary carbon balance and late Holocene carbon accumulation in a northern
686 peatland. Global Change Biology 13: 397-411.
687 Schmidt O, Horn MA, Kolb S & Drake HL (2015) Temperature impacts differentially on the
688 methanogenic food web of cellulose-supplemented peatland soil. Environ Microbiol 17:
689 720-734.
690 Serkebaeva YM, Kim Y, Liesack W & Dedysh SN (2013) Pyrosequencing-based assessment
691 of the bacteria diversity in surface and subsurface peat layers of a northern wetland,
692 with focus on poorly studied phyla and candidate divisions. PloS One 8: e63994.
693 Shen R-C, Xu M, Chi Y-G, Yu S & Wan S-Q (2014) Soil Microbial Responses to
694 Experimental Warming and Nitrogen Addition in a Temperate Steppe of Northern
695 China. Pedosphere 24: 427-436.
696 Sinclair L, Ahmed O, Bertilsson S & Eiler A (2015) Microbial community composition and
697 diversity via 16S rRNA gene amplicons: evaluating the Illumina platform. PloS One 10:
698 e0116955.
699 Sundberg C, Al-Soud WA, Larsson M, Alm E, Shakeri Yekta S, Svensson BH, Sorensen SJ
700 & Karlsson A (2013) 454-Pyrosequencing Analyses of Bacterial And Archaeal
701 Richness In 21 Full-Scale Biogas Digesters. FEMS Microbiology Ecology 85: 612-626.
702 Tully BJ, Wheat CG, Glazer BT & Huber JA (2018) A dynamic microbial community with
703 high functional redundancy inhabits the cold, oxic subseafloor aquifer. ISME J 12: 1-16.
704 Turetsky MR, Kotowska A, Bubier J*, et al.* (2014) A synthesis of methane emissions from 71
705 northern, temperate, and subtropical wetlands. Global Change Biology 20: 2183-2197.
706 Turunen J, Tomppo E, Tolonen K & Reinikainen A (2002) Estimating carbon accumulation
707 rates of undrained mires in Finland–application to boreal and subarctic regions. The
708 Holocene 12: 69-80.
709 Tveit A, Schwacke R, Svenning MM & Urich T (2013) Organic carbon transformations in
710 high-Arctic peat soils: key functions and microorganisms. ISME J 7: 299-311.
711 Wang M & Moore TR (2014) Carbon, nitrogen, phosphorus, and potassium stoichiometry in
712 an ombrotrophic peatland reflects plant functional type. Ecosystems 17: 673-684.
713 Wiedermann MN, Nordin A, Gunnarsson U, Nilsson MB & Ericsson L (2007) Global change
714 shifts vegetation and plant-parasite interactions in a boreal mire. Ecology 88: 454-464.

Yu ZC (2012) Northern peatland carbon stocks and dynamics: a review. Biogeosciences 9: 4071-4085.

Zeng J, Liu X, Song L, Lin X, Zhang H, Shen C & Chu H (2016) Nitrogen fertilization directly affects soil bacterial diversity and indirectly affects bacterial community composition. Soil Biology and Biochemistry 92: 41-49.

Zhou J, Guan D, Zhou B*, et al.* (2015) Influence of 34-years of fertilization on bacterial communities in an intensively cultivated black soil in northeast China. Soil Biology and Biochemistry 90: 42-51.

765 **Table 1** Statistical tests for the 16S rRNA gene sequences, 16S rRNA sequences and protein
766 families derived from the metagenome (PFAM) in relation to the treatments and the
767 standardized depths: above the growing season water table (AWT), around the growing
768 season mean water table (WT), and below the growing season mean water table (BWT).
769 PFAMs were only analysed at the AWT and BWT depths. N, S and GH refer to the main
770 treatment effects of nitrogen, sulfur and greenhouse, and NxS, NxGH and SxGH refer to their
771 two-way interactions, while NxSxGH represents the three-way combination. Only R2-values
772 from the significant results of a permutational multivariate analysis of variance
773 (PERMANOVA) are presented. Similar for the alpha-diversity, only Pielou (evenness index)
774 and Chao (richness index) are represented from the significant results of an ANOVA.

Data		Effect	Standardized depth		
			AWT	WT	BWT
Beta-diversity	16S rRNA gene	N	0.25***	0.18**	0.08***
		S	ns	0.06*	0.03*
		GH	0.07*	0.09**	0.05***
		NxS	ns	0.05*	ns
		NxGH	0.06*	0.05*	ns
		SxGH	ns	ns	0.03*
		NxSxGH	0.05*	ns	0.03*
	16S rRNA	N	0.15**	0.12*	0.09***
		S	ns	0.07*	0.04**
		GH	ns	0.06*	0.05**
		NxS	ns	0.05*	0.03*
		NxGH	ns	ns	ns
		SxGH	ns	ns	ns
		NxSxGH	ns	ns	ns
Functional potential	PFAM	N	ns		0.14*
		S	ns		ns
		GH	ns		ns
		NxS	ns		ns
		NxGH	ns		ns
		SxGH	ns		0.13*
		NxSxGH	ns		ns
Alpha-diversity	16S rRNA gene	N	Pielou*	Chao*;Pielou**	ns
		S	ns	Chao**	Chao**;Pielou*
		GH	ns	ns	Chao*
		NxS	ns	Pielou*	ns
		NxGH	ns	ns	ns
		SxGH	ns	Chao**;Pielou**	ns
		NxSxGH	ns	ns	Pielou*
	16S rRNA	N	ns	ns	ns
		S	ns	ns	Chao*;Pielou*
		GH	ns	ns	ns
		NxS	ns	ns	ns
		NxGH	ns	ns	ns
		SxGH	ns	ns	ns
		NxSxGH	ns	ns	ns

775 Significances codes are: *** $p \leq 0.001$, ** $p \leq 0.01$ and * $p \leq 0.05$. ns denotes non-significant
776 results.

Table 2 Co-variation between taxonomic composition and process data (methane production and oxidation) assessed by fitting the process data onto an ordination derived from a non-metric multidimensional scaling (NMDS), for every standardized depth (AWT: above the growing season mean water table, WT: around the growing season water table (WT), and BWT: below the growing season mean water table).

Data	Standardized depth	NMDS stress value	R2	Significance
16S rRNA - CH_4 production	AWT	0.12	0.35	0.02
	WT	0.09	0.39	0.017
	BWT	0.06	0.51	0.004
16S rRNA gene -CH_4 production	AWT	0.07	0.34	0.0026
	WT	0.09	0.20	ns
	BWT	0.12	0.30	ns
16S rRNA - CH_4 oxidation	AWT	0.12	0.33	ns
	WT	0.09	0.01	ns
	BWT	0.06	0.43	0.016
16S rRNA gene -CH_4 oxidation	AWT	0.07	0.05	ns
	WT	0.09	0.31	ns
	BWT	0.12	0.42	0.006

ns denotes non-significant results.

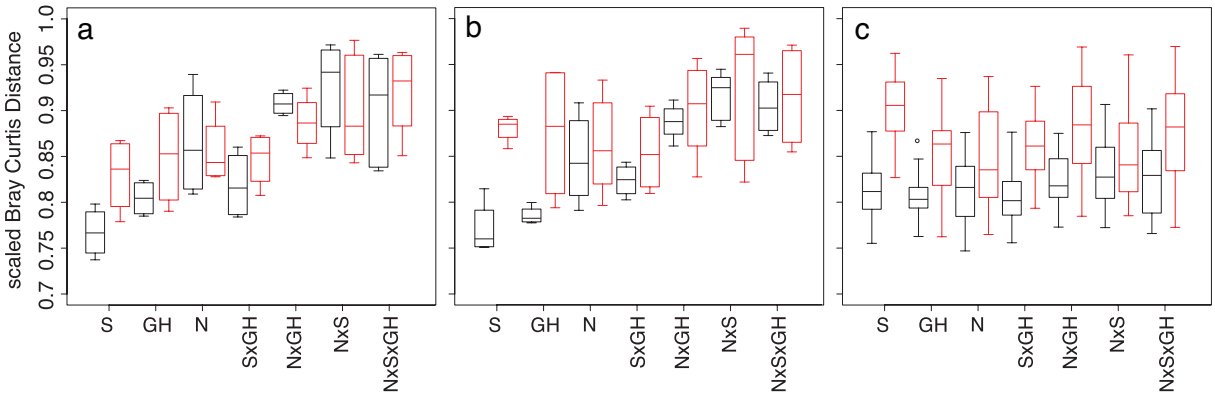

Fig. 1 Prokaryote community composition (β-diversity) turnover in relation to the low treatment levels. a: above the growing season mean water table level. b: around the growing season mean water table level. c: below the growing season mean water table level. Black: community composition derived from the 16S rRNA gene. Red: community composition derived from the 16S rRNA. A Bray-Curtis distance of 0 indicates a complete overlap in community composition between the high and low treatment levels, while a Bray-Curtis distance of 1 indicates complete dissimilarity. Note that the scale on the y-axes starts at 0.7. The number of replicates for the main, two- and three-way interaction effects are 8, 4 and 2, respectively.

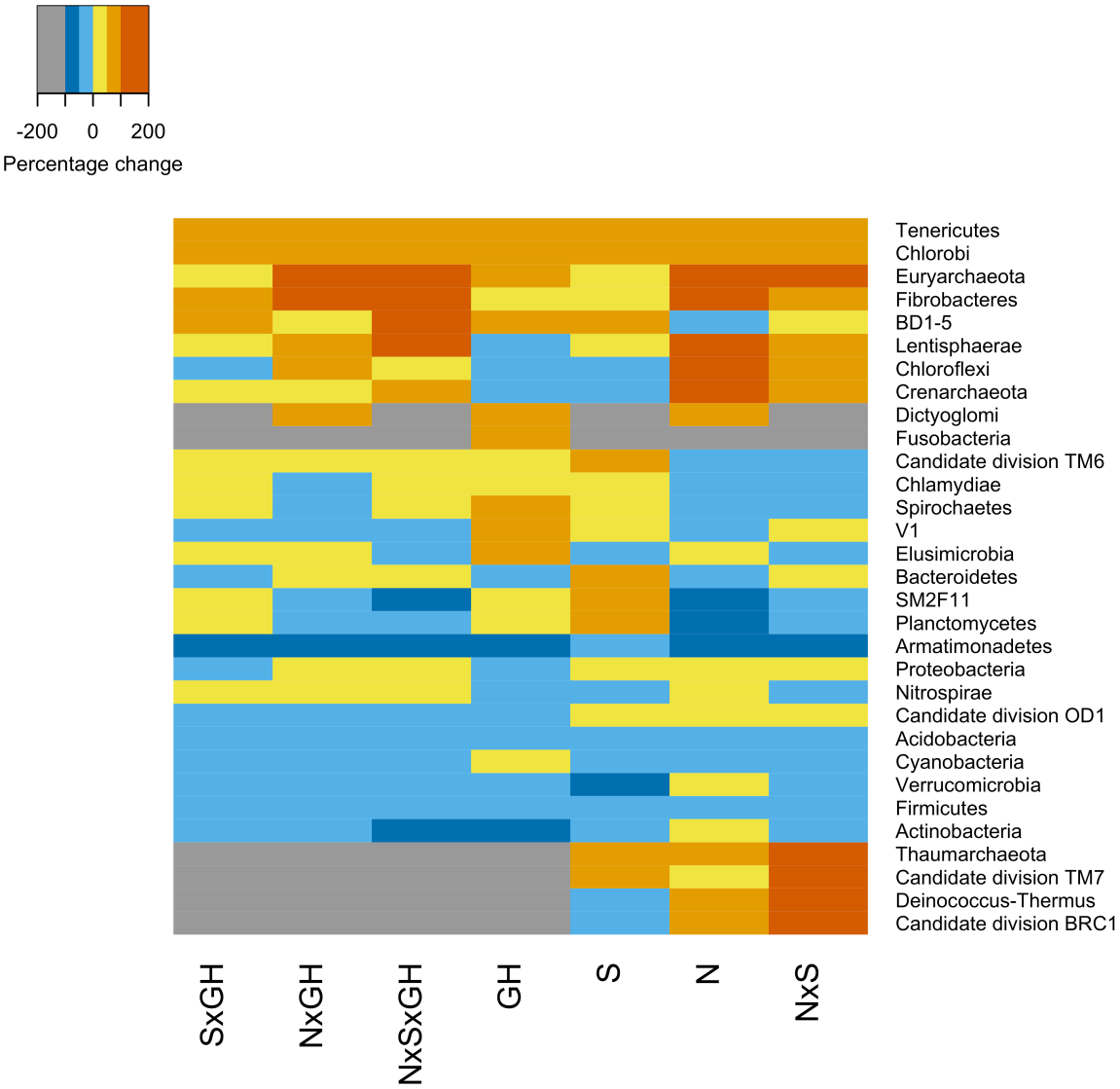

Fig. 2 Relative change in the abundance of the 16S rRNA-derived phyla comparing the high level and the low level treatments, i.e. the relative abundance of each phylum at the high level was subtracted by the corresponding value for the low level and then divided with the low level value. Grey colour shows the phyla that disappeared with the high level treatment and red colour shows the phyla that appeared with the high level treatment. N, S and GH refer to the main treatment effects of nitrogen, sulfur and greenhouse, and NxS, NxGH and SxGH refer to their two-way interactions, while NxSxGH represents the three-way combination.

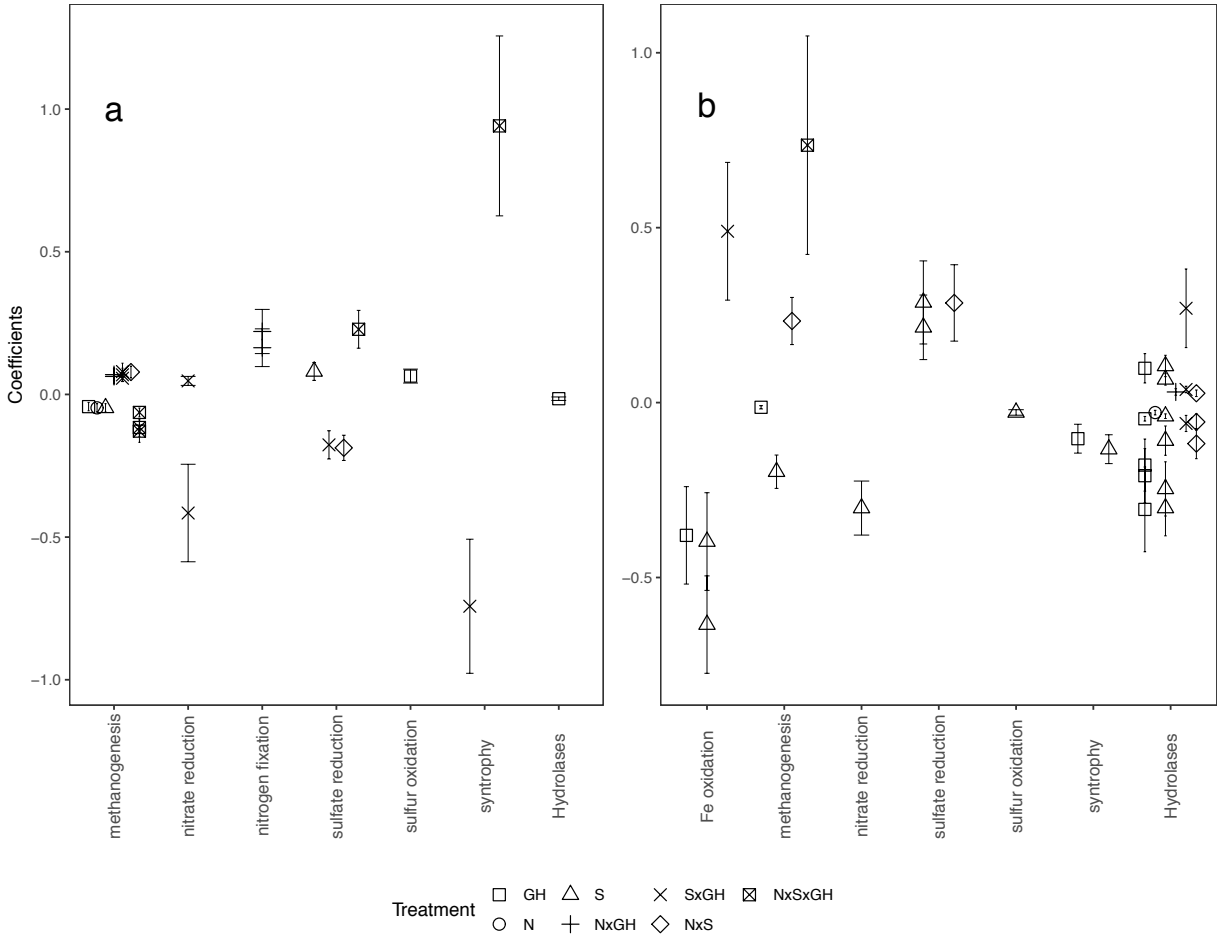

865
866
867 **Fig. 3** Generalized linear models (GLMs) on PFAMs (protein families) related to key steps
868 in the anaerobic degradation of organic matter or relevant to the N and S cycling, at above the
869 water table (AWT; panel a) and below the water table (BTW; panel b). The treatment
870 responses are indicated by the coefficient, showing a decrease or increase in genome
871 equivalents of each individual key PFAM. Only significant treatments responses are shown.
872 Interaction terms in the regression models and the relationships among the variables in the
873 model should be interpreted in as follows: positive coefficient in the case of interactions
874 indicates a synergistic effect when combining perturbations, while a negative coefficient
875 indicates an antagonistic effect, which can even lead to no expression of the perturbations.
876